Determining the Plio-Quaternary uplift of the southern French massif-Central; a new insights for intraplate orogen dynamics.

Oswald Malcles[1], Philippe Vernant[1], Jean Chéry[1], Pierre Camps[1], Gaël Cazes[2,3], Jean-François Ritz[1], David Fink[3].

[1] Geosciences Montpellier, CNRS-University of Montpellier, Montpellier, France

[2] SEES, University of Wollongong, Wollongong, Australia

[3] Australian Nuclear Science and Technology Organisation, Lucas Heights, Australia

Correspondence to: Oswald Malcles (oswald.malcles@umontpellier.fr)

Abstract.

The evolution of intra-plate orogens is still poorly understood. Yet, this is of major importance for understanding the Earth and plate dynamics, as well as the link between surface and deep geodynamic processes. The French Massif Central is an intraplate orogen with a mean elevation of 1000 m, with the highest peak elevations ranging from 1500 m to 1885 m. However, active deformation of the region is still debated due to scarce evidence either from geomorphological or geodetic and seismologic data. We focus our study on the southern part of the Massif-Central, known as the Cévennes and Grands Causses, which is a key area to study the relationship between the recent geological deformation and landscape evolution. This can be done through the study of numerous karst systems with trapped sediments combined with the analysis of a high-resolution DEM.

Using the ability of the karst to durably record morphological evolution, we first quantify the incision rates. We then investigate tilting of geomorphological benchmarks by means of a high-resolution DEM. We finally use the newly quantified incision rates to constrain numerical models and compare the results with the geomorphometric study.

We show that absolute burial age ($^{10}Be/^{26}Al$ on quartz cobbles) and the paleomagnetic analysis of karstic clay deposits for multiple cave system over a large elevation range correlate consistently. This correlation indicates a regional incision rate of 83 $^{+17}/_{-5}$ m/Ma during the last ca 4 Myrs (Pliocene-Quaternary). Moreover, we point out through the analysis of 55 morphological benchmarks that the studied region has undergone a regional southward tilting. This tilting is expected as being due to a differential vertical motion between the north and southern part of the studied area.

Numerical models show that erosion-induced isostatic rebound can explain up to two-thirds of the regional uplift deduced from the geochronological results and are consistent with the southward tilting derived from morphological analysis. We presume that the remaining unexplained uplift is related to dynamic topography or thermal isostasy due to the Massif Central Pliocene-Quaternary magmatism.

Integrating both geochronology and morphometrical results into lithospheric-scale numerical models allows a better understanding of this intraplate-orogen evolution and dynamic. We assume that the main conclusions are true to the general case of intraplate deformation. That is to say, once the topography has been generated by a triggering process, rock-uplift is then enhanced by erosion and isostatic adjustment leading to a significant accumulation of mainly vertical deformation.

1 Introduction and Tectonic Setting

1.1 Introduction

Since the past few decades, plate-boundary dynamic is, to a first order, well understood. This is not the case for intraplate regions, where short-term (10^3-10^5 yr) regional strain rates are low and the responsible dynamical processes are still in debate (e.g. Calais et al., 2010; Vernant et al., 2013; Calais et al., 2016; Tarayoun et al., 2017). Intraplate deformations evidenced by seismic activity is sometimes explained by a transient phenomenon (e.g., glacial isostatic rebound, hydrological loading). However, to explain the persistence through time of intraplate deformation, and explain the high finite deformation we can observe in the topography in many parts of the world as for instance the Ural mountains in Russia, the Blue Mountains in Australia or the French Massif Central, one needs to invoke continuous processes at the geological time-scale.

Located in the southwestern Eurasian plate (Fig. 1), the French Massif Central is an ideal case to study this processes because a high resolution DEM encompasses the whole region and widespread karstic areas are present along its southern and western edges, allowing the possibility to quantify landscape evolution rates thanks to TCN burial ages. The region is characterized by a mean elevation of 1000 m with summits higher than 1500 m. Such topography is likely to be the result of recent, active uplift and as the Cevennes mountains experiences an exceptionally high mean annual rainfall (the highest peak, Mount Aigoual, records the highest mean annual rainfall in France of 4015 mm) it raises the question of a possible link between erosion and uplift as previously proposed for the Alps (Champagnac et al., 2007; Vernant et al., 2013; Nocquet et al., 2016). This region currently undergoes a small but discernible deformation, but no significant quantification can be deduced due to the scarcity in seismicity (Manchuel et al., 2018). In addition, GPS velocities are below the uncertainty threshold of GPS analyses (Nocquet et Calais, 2003; Nguyen et al., 2016).

In this study we focus on the Cevennes Mountains and the Grands Causses (Fig.1) area, where cave systems with trapped sediments are known over a widespread altitude range. South and West of the crystalline Cevennes mountains, prominent limestone plateaus, named Grands Causses, rise to 1000m and are dissected by few canyons that are several hundreds of meter deep. The initiation of incision, its duration and the geomorphic processes leading to the present-day landscape remain poorly constrained. A better understanding of the processes responsible for this singular landscape would bring valuable information on intraplate dynamics, especially where large relief exists.

1.2. Geological background

The oldest rock units in the study area were formed during the Variscan orogeny (late Palaeozoic, ~300 Ma; Brichau et al., 2007) and constitute the crystalline basement of the Cevennes. Between 200 and 40 Ma (Mesozoic and middle Cenozoic), the region was mainly covered by the sea ensuring the development of an important detrital and carbonate sedimentary cover, which can reach several km of thickness in some locations (Sanchis and Séranne, 2000; Barbarand et al., 2001). During the Mesozoic

era, an episode of regional uplift and subsequent erosion and alteration (called the Durancian event) is proposed for the origin of the flat, highly elevated surface that persists today across the landscape (Bruxelles, 2001; Husson, 2014).

The area is affected by the major NE-SW trending Cevennes fault system, a lithospheric-scale fault, inherited from the Variscan orogen. This fault system was reactivated several times (e.g. as a strike-slip fault during the Pyrenean orogen or as a normal fault during the Oligocene extension). During the Pyrenean orogeny, between 85 to 25 Ma (Tricart, 1984; Sibuet et al., 2004), several faults and folds systems affected the geological formations south of the Cevennes fault, while very few deformations occurred farther north within the Cévennes and Grand Causses areas (Arthaud and Laurent, 1995). Finally, the Oligocene extension (~30 Ma) led to the counterclockwise rotation of the Corso-Sardinian block and the opening of the Gulf of Lion, re-activating some of the older compressive structures as normal faults. The main drainage divide between the Atlantic Ocean and the Mediterranean Sea is located in our study area and is inherited from this extensional episode (Séranne et al., 1995; Sanchis et al., 2000).

Afterwards during the Pliocene-Quaternary period, an intense volcanic activity has affected the region, from the Massif Central to the Mediterranean shoreline. This activity is characterized by several volcanic events that are well constrained in age (Dautria et al., 2010). The last eruption occurred in the Chaîne des Puys during the Holocene (i.e. the past 10 kyrs (Nehlig et al., 2003; Miallier et al., 2004). Some authors proposed that this activity is related to a hotspot underneath the Massif Central leading to an observed positive heat-flow anomaly and a possible regional Pliocene-Quaternary uplift (Granet et al., 1995; Baruol and Granet, 2002). Geological mapping at different scale can be found at: http://infoterre.brgm.fr/.

Despite this well described overall geological evolution the onset of active incision that has shaped the deep valleys and canyons (e. g. Tarn or Vis river, Fig 1) across the plateaus, and the mechanisms that controlled this incision are still debated. One hypothesis proposes that canyon formation was driven by the Messinian salinity crisis with a drop of more than 1000 m in Mediterranean Sea level (Moccochain, 2007). This, however, would then not explain the fact that the Atlantic watersheds show similar incision. Other studies have suggested that the incision is controlled by the collapse of cave galleries that lead to fast canyon formation mostly during the late Quaternary, thus placing the onset of canyon formation only a few hundreds of thousands of years ago (Corbel, 1954). More recently, it has been proposed (based on relative dating techniques and sedimentary evidence) that incision during the Quaternary was negligible (i.e. less than a few tens of meters), and that the regional morphological structures seen today occurred around 10 Ma (Séranne et al., 2002; Camus, 2003).

1.3 Materials and methods

In this paper, we provide new quantitative constraints on both the timing of incision and the rate of river down-cutting in the central part of the Cévennes and of the Grands Causses that has resulted in the large relief between plateau and channel bed.

We employ two methods to infer allochthonous karstic infilling age and associated river down-

cutting. First, we use quartz cobbles to measure concentration of cosmogenic ^{10}Be and ^{26}Al isotopes. The $^{10}Be/^{26}Al$ ratio provide burial ages of these karstic infilling. Second, paleomagnetic analyses of clay deposits to obtain paleo-polarities. In both cases, vertical profiles among tiered caves systems and horizontal galleries could provide local incision rate information. By analyzing a high-resolution DEM (5m), we show that the region is affected by a southeastward regional tilting. Our results allow to quantify the role of the Pliocene-Quaternary incision on the Cévennes landscape evolution and to constrain numerical modeling from which we derive the regional uplift rates and a tilt of geomorphological markers.

If incision is initiated by uplift centered on the North of the area where elevations are maximum, it will lead to tilting of fossilized topographic markers as strath terraces. Our research approach provides an opportunity to discriminate between three possible explanations for the current terrain morphology. The first is based on old uplift and old incision (Fig. 2A). In this case, apparent incision rates would be very low. For instance, if incision commenced 10 Ma (Serrane et al., 2002), we would find surface tilting but cosmogenic burial dating with $^{10}Be/^{26}Al$ which cannot discern ages older than ~ 5Ma due to excessive decay of 26Al, would not be possible. The second possibility (Fig. 2B) is that the uplift is old, and incision consequently follows but with a time lag. Here the incision rate would be rather fast, but no tilting is expected for the river-related markers because no differential uplift occurs after their formation. Finally, the third possibility (Fig 2C) is that uplift and incision are concurrent and recent (i.e. within the time scale of cosmogenic burial dating) and thus we would expect burial ages < 5 Myrs relatively high incision rates, and tilting of morphological markers. These different proposals for the temporal evolution of the region will then be compared using numerical modeling.

2. Determining the incision rates in the Cévennes and the Grand Causses Region

2.1. Principles and methods

2.1.1. Karst model

No evidence of important aggradation events has been reported in the literature for the studied area. Therefore, we base our analysis on a per descensum infill model of the karst networks whereby sediments are transported and then deposited within cave galleries close to base level. When cave-systems and entry passages are near the contemporaneous river channel elevation (including higher levels during floods), the deposition into caves of sediments, from clay to cobbles occurs, especially during flood events. Subsequent river incision into bedrock creates a relative base level drop (due to uplift or sea-level variations). The galleries associated with the former base-level are now elevated above the new river course and become disconnected from further deposition. Hence fossilised and trapped sediments throughout the cave network represent the cumulative result of incision. In this commonly used model (Granger et al., 1997; Audra et al., 2001; Stock et al., 2005; Harmand et al., 2017), the higher the gallery elevation (relative to the present-day base level) the older the deposits in that gallery. As a result, the objective here is to quantify a relative lowering of the base level in the

karst systems, with the sediments closest to the base level being the youngest deposits, and note that we do not date the cave network creation which may very well pre-date river sediment deposition. Within individual canyons, successions of gallery networks across the full elevation range from plateau top to modern river channel, were not always present and often sampling could not be conducted in a single vertical transect. Thus, we make the assumption of lateral altitudinal continuity i.e. that within a watershed, which may contain a number of canyons, the sediments found in galleries at the same elevation were deposited at the same time. Inside one gallery, we use the classical principle of stratigraphy sequence (i.e. the older deposits are below the younger ones). More informations and detailed relationships concerning the karstic development and geometric relationship between karstic network and morphological markers could be find in Camus (2003). In any cases, our aim is not to date the galleries formation, neither to explain the formation processes (e.g. past preferential alteration layer); but to use the time information brought by the sediment that have been trapped into the cave system. Therefore, we apply the common used model (example in Harmand et al., 2017) that had been proved by Granger et al., (1997, 2001). For cave topographic survey, we refer the reader to https://data.oreme.org/karst3d/karst3d_map that provides 3D survey.

2.1.2. Burial ages

Burial dating using Terrestrial cosmogenic nuclides (TCN) is nowadays a common tool to quantify incision rates in karstic environment (Granger and Muzikar, 2001; Stock et al., 2005; Moccochain., 2007; Tassy et al., 2013; Granger et al., 2015; Calvet et al., 2015; Genti, 2015; Olivetti et al., 2016; Harmand et al., 2017; Rovey II et al., 2017; Rolland et al., 2017; Sartégou, 2017; Sartégou et al., 2018). This method relies on the differential decay of TCN in detrital rocks that were previously exposed to cosmic radiation before being trapped in the cave system. With this in mind, the ^{10}Be and ^{26}Al nuclide pair is classically used as (i) both nuclides are produced in the same mineral (i.e. quartz), (ii) their relative production ratio is relatively well constrained (we use a standard ^{26}Al/^{10}Be pre-burial ratio of 6.75, see Balco et al., 2008) and (iii) their respective half-lives (about 1.39 Myr and 0.70 Myr for ^{10}Be and ^{26}Al, respectively) are well suited to karstic and landscape evolution study, with a useful time range of ~100 ky to ~5 Myr.

To quantify the incision rate of the limestone plateau of the Cevennes area, we analysed quartz cobbles infilling from four caves of the Rieutord canyon (Fig. 1), this canyon is well suited for such study because horizontal cave levels are tiers over 200 m above the current river-level and are directly connected to the canyon, leading to a straight relationship between river elevation and the four cave infilling that we have sampled (Cuillère cave, Route cave, Camp-de-Guerre cave and Dugou cave). Furthermore, cobbles source is well known and identified: the upstream part of the Rieutord river, some tens of kilometers northward, providing a unique sediment origin composed of granite and metamorphic rocks embedding numerous quartz veins. All samples (Example Fig. 3) were collected far enough away (>20m) from the cave entrance and deep enough below the surface (>30m) to avoid secondary in-situ cosmogenic production of ^{10}Be and ^{26}Al in the buried sediments.

The quartz cobbles were first crushed and purified for their quartz fraction by means of sequential acid attack with Aqua-Regia (HNO_3 +3HCl) and diluted Hydrofluoric acid (HF). Samples were then prepared according to ANSTO's protocol (see Child et al. 2000) and ~300µg of a ^{9}Be carrier solution was added to the purified quartz powder before total dissolution. AMS measurements were performed on the 6MV SIRIUS AMS instrument at ANSTO and results were normalised to KN-5-2 (for Be, see Nishiizumi et al., 2007) and KN-4-2 (for Al) standards. Uncertainties for the final ^{10}Be and ^{26}Al concentrations include AMS statistics, 2% (Be) and 3% (Al) standard reproducibility, 1% uncertainty in the Be carrier solution concentration and 4% uncertainty in the natural Al measurement made by ICP-OES, in quadrature. Sample-specific details and results are found in table 1.

2.1.3. Paleomagnetic analysis

In parallel with burial dating, we analyzed the paleomagnetic polarities within endokarstic clay deposits within two main cave systems: the *Grotte-Exsurgence du Garrel* and the *Aven de la Leicasse* (Fig. 1). These two cave systems allowed us collecting samples along a more continuous range of elevations than the one provided by the Rieutord samples (for burial age determination) and also extending the spatial coverage to the Southern Grands Causses region. Thanks to the geometry of these two cave systems, we sampled a 400m downward base level variation. The sampling was done along vertical profiles from a few ten of centimeters to 2 meters high by means of Plexiglas cubes with a 2 cm edge length (Fig. 4) used as a pastry cutter. We weren't able to analyse clay samples from Rieutord canyon because no reliable clay infilling was found in the Rieutord caves.

Demagnetisation was performed with an applied alternative field up to 150mT using a 2G-760 cryogenic magnetometer, equipped with the 2G-600 degausser system controller. Before this analysis, each sample remained at least 48h in a null magnetic field, preventing a possible low coercivity viscosity overprinting the detrital remanent magnetisation (DRM) (Hill, 1999; Stock et al., 2005; Hajna et al., 2010). If the hypothesis of instantaneous locked in DRM seems reasonable compared with the studied time span, it is important to keep in mind that the details of DRM processes (as for instance the locked in time) is not well understood (Tauxe et al., 2006; Spassov et Valet, 2012) and could possibly lead to small variations (few percents) in the following computed incision rates.

Because fine clay particles are expected being easily reworked in the cave, careful attention was paid to the site selection and current active galleries were avoided. Clays deposits had to show well laminated and horizontal layering in order to prevent analysis of in-situ produced clays (from decalcification) or downward drainage by an underneath diversion gallery that could strongly affect the obtained inclination (and also the declination to a minor extent). Note that for paleo-polarities study alone, small inclination or declination variations won't result in false polarities

2.2 Quantifying the average incision rates

2.2.1. Local incision rate from burial ages (Rieutord Canyon)

The relationship between burial ages and incision is shown in Figure 5. For the four caves, we observed a good relationship between burial ages and finite incision, except for the Camp-de-Guerre cave (CDG) site, the higher the cave is, the older the burial ages are. Burial ages for the Cuillère cave, Dugou cave, Camp-de-Guerre cave and Route cave are 2.16 ± 0.15, 0.95 ± 0.14, 0.63 ± 0.1 and 0.21 ± 0.1 Myrs respectively. This is consistent with the supposed cave evolution and first-order constant incision of the Rieutord canyon. CDG age has to be considered with caution. The CDG cave entrance located in a usually dry thalweg can act as a sinkhole or an overflowing spring depending on the intensity of the rainfall. The sample was collected in a gallery showing evidence of active flooding ~10 m above the Rieutord riverbed, therefore the older than expected age, given the elevation of the cave, is probably due to cobbles that came from upper galleries during flood events. Forcing the linear regression to go through the origin, leads to an incision rate of 83 ± 35 m/Ma. These results show that at least half of the 300 m deep Rieutord Canyon is a Quaternary incision. Extrapolating the obtained rate yields an age of 4.4 ± 1.9 Ma for the beginning of the canyon incision, which suggests that the current landscape has been shaped during the Pliocene-Quartenary period. To extend our spatial coverage and bring stronger confidence into our results, we combine Rieutord burial ages with paleomagnetic data from watersheds located on the other side of the Herault watershed.

2.2.2. Local incision rate from paleomagnetic data (Southern Grands Causses)

A total of 100 clay-infilling samples distributed over of 13 sites (i.e. profiles) was studied. The lowest sample elevation above sea level (a.s.l.) is in the Garrel (ca 190 m) and the highest in the Leicasse (ca 580 m a.s.l.). In the Leicasse cave system, we sampled 8 profiles totalizing 60 samples. Profiles elevations are located between ca 200 m and ca 400 m above the base level (a.b.l.), which corresponds to the elevation of the Buèges river spring at 170 m a.s.l.

In the Garrel cave system, we sampled 5 profiles for a total of 40 samples that range between 20 m and 80 m a.b.l. defined by the Garrel spring at 180 m a.s.l. Given the very marginal difference in elevation between the local base levels from these two caves, we assume that they have the same local base level. At each studied site, if all the profile samples have the same polarity, the site is granted with the same polarity, either normal or reverse. If not (i.e. the profile displays normal and reverse polarities), we consider it as a transitional site. Figure 6 shows the results plotted with respect to the paleomagnetic scale (x axis) for the past 7 Ma, and their elevation above the base level (y axis). The measured paleomagnetic polarities on each site is plotted several times for given incision rates supposed to be constant through times (this allows determining different age models and analyze their correlation with the distribution of paleomagnetic data, see below). First, we note a good agreement between samples located at the same elevation elevation and being part of the same stratigraphic layer (Camus, 2003). This syngenetic deposition allows, as best explanation to prevent from a possible partial endokarstic reworking. Second, the different elevations of the galleries where we collected the samples allow proposing that the Leicasse deposits encompass at least three chrons, while the Garrel deposits encompass only one. Third, a transitional signal comprised between a reversal signal (lower

samples) and a normal signal (upper ones) is observed at Les Gours sur Pattes (LGP) sampling site (Fig. 7). This provides a strong constraint on the age of the sediment emplacement in the Leicasse with respect to the magnetostratigraphic timescale (Fig. 6).

Compared to the Leicasse cave system, the elevation/polarity results for the Garrel are less constrained. Only one site shows a reverse polarity at 90 m a.b.l., and the transitional polarity found at 40 m a.b.l. is unclear (tab, suppl mat.). The rest of the polarities (72 samples) are all normal. Given that a U-Th ages younger than 90 kyrs was obtained for two speleothems (Camus, 2003) covering our samples collected at 40 m a.b.l. (Fig. 6), we consider that the emplacement of the clay deposits occurred during the most recent normal period and are therefore younger than 0.78 Ma (Figure 6). The transition between the highest normal sample and the reversed one is located somewhere between 78 m and 93 m a.b.l. suggesting a maximum base level lowering rate of 109 ± 9 m/Ma.

To go further in the interpretation of our data, and better constraint the incision rate, we performed a correlation analysis between observed and modeled polarities for a 0 to 200 m/Ma incision-rate range (linear rate, each 1 m/Ma). Modeled polarities are found using the intersection between sample elevation and incision-rate line.

We obtained 10 possible incision rates with the same best correlation factor (Fig. 8) spanning from 43 to 111 m/Ma (mean of 87 ± 24 m/Ma). Taking into account the transitional signal of the LGP site in the Leicasse cave yields a linear incision rate of 83 $^{+17}/_{-5}$ m/Ma. Proposed uncertainties are based on previous and next transition-related estimated incision rate.

Using a similar approach for the Rieutord crystalline samples, that is to say we compute, for the same incision-rate space, the distance in a least square sens between the modeled age and the measured ones in order to check the cost function shape and acuteness. With this method, we determined a linear incision rate of 85 ± 11 m/Ma (Fig 8). Those two results, based on independent computations, suggest the same first-order incision rate for the last 4 Ma of 84 $^{+21}/_{-12}$ m/Ma. Given that the Rieutord, Garrel and Buèges rivers are all tributaries of the Hérault river, we propose that this rate represents the incision rate for the Hérault river watershed, inducing approximately 300-350 m of finite incision over the Pliocene-Quaternary period.

If the landscape is at first order in an equilibrium state, that is to say, if we preclude our incision rates being a regressive erosional signal, the incision needs to be balanced by an equivalent amount of uplift. If the uplift rate is roughly correlated to the regional topography, lowest uplift rates would be expected in the south of our sampling sites inducing regional tilting of morphological benchmarks. In the next part, we search for such evidences that would suggest differential uplift.

3 Geomorphometric signature

3.1 Tested hypothesis and methods

According to the Massif-Central centered uplift hypothesis, morphological markers such as strath

299 terraces, fluvio-karstic surfaces or abandoned meanders should display a southward tilting due to
300 differential uplift between the northern and the southern part of the region.

301 To investigate these differential vertical movement signals, we used the morphological markers
302 available in the study area (Fig. 9). We used a 5 m resolution DEM analysis to identify the markers
303 corresponding to surfaces with slope < 2°. This cut-off slope angle prevents to identify surface related
304 to local deformation such as for example landslide or sinkhole. We point out that surface slope
305 increase through time (e.g. apparent tilting) could be due to diffusion processes and not related to
306 differential vertical displacements. However that problem is address by 1) the automatic selection and
307 correction and the final manual check for residue random distribution (see below).The local river
308 slope is on the order of 0.1° so the 2° cut-off angle is far from precluding to identify tilted markers.
309 We also use a criterion based on an altitudinal range for a surface. This altitudinal span is set
310 individually for each surface based on elevation, slope and curves map analysis, and encompass from
311 few meters to tens of meters depending on the size of the marker. We checked 80% of the identified
312 surfaces in the field in order to avoid misinterpretation. Some pictures are provided in supplementary
313 material. The dip direction and angle of the surface in computed in a two steps approach. First, we fit
314 a plan using extracted points from the DEM inside the delimited surface. Second, based on this plan
315 we remove the DEM points with residuals 3 times larger than the standard error and compute more
316 accurate plan parameters (second fitting). This outlier suppression removes any inaccurate DEM
317 points and correct for inaccurate surface delimitation (e.g. integration of a part of the edge of a strath
318 terrace, diffusion processes marks, etc.).
319 Because no obvious initially horizontal markers are known, we propose to correct the marker current
320 slope by the initial one to quantify the tilt since the marker emplacement. To do so we follow the
321 method used by Champagnac et al. (2008) for the Forealps. We identify the drain related to the marker
322 formation and compute its current local slope and direction. This method assumes that landscapes are
323 at the equilibrium state and that the river slope remained constant since the marker formation. This
324 assumption seems reasonable given the major river profiles and because most of the markers used are
325 far from the watershed high altitude areas precluding a recessive erosional signal. Finally, we
326 removed the local river plan from the DEM extracted surface.
327
328 3.2. Morphometrical results
329 Following this methodology, we obtained 61 surfaces (e.g. strath terraces). We then applied three
330 quality criterions to ensure the robustness of our results: 1) The minimal surface considered is 2500
331 m^2 based on a comparison between the 5m resolution DEM and a RTK GPS survey over 3 strath
332 terraces (Hérault river); 2) Final plans with dip angles larger than 2° are removed; 3) The residuals for
333 each geomorphological marker must be randomly distributed without marker edge signal, or clear
334 secondary structuration. Only 38 markers meet those 3 quality criterions.
335 If the identified and corrected markers have indeed registered a differential uplift between the north
336 and the south, we expected the following signals:

- The dipping direction of the tilted markers should be parallel to the main gradient of the topography, i.e. between 150°E and 180°E for our studied region. This expectation is the most important one, regarding uncertainties on the uplift rate and lithospheric elastic parameters.

- A latitudinal tilting trend, i.e. an increase of the tilt angle along the topography gradient. Indeed, null or small tilts are expected near the shoreline and within the maximum uplift area of the Cevennes/Massif Central, while the maximum tilt is expected at a mid-distance between these two regions, i.e. about 50 km inland from the shoreline.

- A positive altitudinal tilting trend (an increase in dip angle with altitude). This trend would be representative of the accumulation of finite tilt. However, it supposes a linear relationship between the altitude and the age of the marker formation. If at first order, this straightforward hypothesis seems reasonable for river-controlled markers (e.g. strath terraces), other surfaces are hardly expected to follow such an easy relationship.

Among the three expected signal, southward dipping is robustly recorded with a mean tilt angle of 0.60 ± 0.40 ° with an azimuth of N128 ± 36°E (Fig. 10). Latitudinal trend and altitudinal trend are less robustly reached but that is not surprising because of the strong susceptibility to local phenomenon or even so lack of robust age constraint.

4 Discussion

Both geomorphological and geochronological evidence suggest a Pliocene-Quaternary uplift of the Cevennes area. The origin of such uplift could be associated with several processes: erosion-induced isostatic rebound, dynamic topography due to mantle convection, thermal isostasy, residual flexural response due to the Gulf of Lion formation, etc. For the Alps and Pyrenees mountains, isostatic adjustment due to erosion and glacial unloading has been recently quantified (Champagnac et al., 2007, Vernant et al., 2013; Genti et al, 2016, Chery et al. 2016). Because the erosion rates measured in the Cevennes are similar to those of the Eastern Pyrenees (Calvet et al., 2015, Sartégou et al., 2018a), we investigate by numerical modeling how an erosion-induced isostatic rebound could impact the southern Massif Central morphology and deformation.

We define a representative cross-section parallel to the main topographic gradient (i.e. NNW-SSE) and close to the field investigation areas (Figure 11). We study the lithospheric elastic response to erosion with the 2D finite element model ADELI (Hassani et Chery, 1996; Chéry et al. 2016). The model is composed of a plate accounting for the elasticity of both crust and uppermost mantle. Although the lithosphere rigidity of the European plate in southern Massif central is not precisely known, vertical gradient temperatures provided by borehole measurements are consistent with heat flow values ranging from 60 to 70 $mW.m^2$ (Lucazeau et Vasseur, 1989). Therefore, we investigate plate thickness ranging from 10 to 50 km as done by Stewart et Watts (1997) for studying the vertical

motion of the alpine forelands.

We choose values for Young's and Poisson parameters of respectively 10^{11} Pa and 0.25, both commonly used values for lithospheric modeling (e.g. Kooi et Cloething, 1992; Champagnac et al. 2007, Chéry et al., 2001). This leads to long-term rigidity of the lithosphere model ranging from 10^{21} to 10^{25} N.m. Since the effect of mantle viscosity on elastic rebound is assumed to be negligible at the time scale of our models (1 to 2 Myrs), we neglect the visco-elastic behaviour of the mantle. Therefore, the base of the model is supported by an hydrostatic pressure boundary condition balancing the weight of the lithosphere (Fig. 11). Horizontal displacements on vertical sides are set to zero since geodetic measurements show no significant displacements (Nocquet et Calais, 2003; Nguyen et al., 2016). The main parameters controlling our model are the erosion (or sedimentation) triggering isostatic rebound and the elastic thickness.

The erosion profile (Fig. 11) is based on topography, our newly proposed incision rate and other studies (Olivetti et al., 2016 for onshore denudation and Lofi et al., 2003; Leroux et al., 2014 for offshore sedimentation). This profile is a simplification of the one that can be expected from Olivetti et al. (2006) and do not aim at matching precisely the published data because of, (i) the explored time-span (~ 1 Myrs) is not covered by thermochronological data (> 10Myrs) or cosmogenic denudation rate (10s-100s kyrs); (ii) we base our erosion rate as being linked with local (10s km^2) slopes, that are higher near the drainage divide. We, by this aim can invoke any kind of erosion processes (e.g. landslides); and (iii) the model assumes a cylindrical structure and consequently, high-frequency lateral variations in term or actual denudation rate or proxy (slope, elevation, etc.) must be averaged. Concerning this erosion profile, parametric study (highest erosion rate ranging from 1 to 1000 m/Ma) give no difference in the interpretation and, for few percent variations, only few percent variations in the modeled uplift-rate.

The flexural rigidity controls the intensity and wavelength of the flexural response and ranges from 10^{21} to 10^{25} N.m. It can be expressed as a variation in elastic thickness (Te) ranging from 4.4 to 96 km (Fig. 12). We also test a possible Te variation between inland and offshore areas. For the following discussion, we use an elastic thickness of 15 km corresponding to a value of D of 3.75 $x10^{23}$ N/m. In this case, the inland and offshore parts are largely decoupled and the large sedimentation rate in the Gulf of Lion does not induce a flexural response on the Cévennes and Grands Causses areas.

With a maximum erosion rate of 80 m/Ma (Fig 11), the models display uplift rates of 50 m/Ma over more than 100 km. As previously explained, the finite incision is permitted by an equal amount of uplift considering that the incision is not due to regressive erosion.

Every models show a general uplift. However, the uplift amplitude are smaller than the expected ones. To obtain the same uplift rate than the incision rates, the applied erosion rate over the model must be increased. However, we assume that the landscape is at equilibrium, so, if the erosion rate is

increased, it will be higher than the incision rate leading to the decay of relief over the area. No evidence of such evolution is found over the region and, if further studies need to be done to quantify the actual erosion rate, we mostly think that a second process is acting, inducing the rest of the uplift that can't be obtained by the erosion–induced isostatic adjustment. Finally, models predict a seaward tilt of the surface at the regional-scale (Fig. 13), in agreement with the observed tilting of morphological markers.

We assume that the sediments collected in the karst were deposited per descensum, i.e. we do not know if the galleries existed a long time before or were formed just before the emplacement of the sediments, but the more elevated the sediments are, the older their deposit is. If there is no evidence of an important aggradation episode leading to more a complex evolution as proposed for the Ardèche canyon (Moccochain et al., 2007; Tassy et al., 2013), we point out that small aggradation or null erosion period could, however, be possible. Some processes could explain such relative stability: e.g. variation in erosion (due to climatic fluctuation) or impact of eustatic variations (in river profile, flexural response, etc.). Such transient variations have been shown for the Alps (Saillard et al., 2014; Rolland et al., 2017) and are proposed as being related to climato-eustatic variations and therefore should last 10 to 100 kyrs at most.

Based on our sampling resolution, we cannot evidence such transient periods and we must use an average base level lowering rate in the karst, which we correlate to the incision of the main rivers. The TCN-based incision rate derived from the Rieutord samples (83 ± 35 m/Ma) is consistent with the one derived from the Garrel (U-Th ages: 85.83 m/Ma according to the sole U/Th exploitable result (Camus, 2003)) and from the Garrel-Leicasse combination (Paleomagnetic approach: $84\ ^{+21}/_{-12}$ m/Ma). This mean incision rate of ca. 85 m/Ma lasting at least 4 Ma, highlights the importance of the Pliocene-Quaternary period into the Cévennes and Grand Causses morphogenesis. Furthermore, the 300 to 400 m of incision precludes a relative base level controlled by a sea-level drop. Indeed, documented sea level variations are less than 100 m (Haq, 1988, Miller et al., 2005). Furthermore, the Herault river does not show any significant knickpoints or evidence of unsteadiness in its profile as expected if the incision was due to eustatic variations. Therefore, we propose that the incision rate of ~85 m/Ma is due to a Pliocene-Quaternary uplift of the Cévennes and Grands Causses region.

Other river-valley processes could lead to a local apparent high incision rate as for instance major landslide or alluvial fan (Ouimet et al., 2008). This hypothesis of an epigenetic formation of the Rieutord is irrelevant because of i) none of the possible causes had been found in the Rieutord canyon and ii) the consistency of the TCN-based incision rate and the paleomagnetic-based incision rate for two other cave-systems. Indeed, the use of two independent approaches and three locations is a good argument in favour of the robustness of our proposed mean 85 m/Ma incision rate. Yet, using more data, particularly burial dating colocalized with clays samples and adding sampling sites would give a stronger statistical validation. In the Lodève basin (Point 4, Fig. 1), inverted reliefs allow another independent way to quantify minimal incision rate. K/Ar and paleomagnetic dated basaltic flows

spanning from 1 to 2 Myrs old that were deposited at the bottom of the former valley (Dautria et al., 2010) are now located at ca 150 m above the current riverbed leading to an average incision rate of 77 ± 10 m/Ma, in agreement with karst-inferred incision rates.

Furthermore, preliminary results from canyons on the other side of the Grands Causses (Tarn and Jonte) based on in-situ terrestrial cosmogenic dating suggest similar incision rates (Sartegou et al., 2018b) and confirm a regional base level lowering of the Cévennes and Grands Causses region during the Pliocene-Quaternary. This is consistent with the similarities of landscapes and lithologies observed both on the Atlantic and Mediterranean watersheds (e.g. Tarn river).

Once the regional pattern of the Pliocene-Quaternary incision established for the Cévennes-Grands Causses area, the next question is how this river downcutting is related to the regional uplift? First order equilibrium shape and absence of major knick points in the main river profiles preclude the hypothesis of regressive erosion. Hence, back to the three conceptual models presented in part 1 (Fig.2), we can discard, at first order, the models A (Old uplift-recent incision) and B (Old uplift-old incision) because obtain incision rate show recent incision and surface tilting tend to prove a current uplift. Therefore, the incision rate has to be balanced to the first order by the uplift rate. We add that eustatic variations are of too low magnitude (100-120 m) and can't explain such total incision (up to 400m). Furthermore, no obvious evidence of active tectonics is reported for the area raising the question of the processes responsible for this regional uplift. Very few denudation rates are reported for our study area (Schaller et al., 2001; Molliex et al., 2016; Olivetti et al., 2017), and converting canyon incision rates into denudation and erosion rates is not straightforward, especially given the large karst developed in the area. Using a first order erosion/sedimentation profile following the main topography gradient direction we have modeled the erosion-induced isostatic rebound. If this process could create between half and two third of the Pliocene-Quaternary uplift, a previously existent topography is needed to trigger erosion so it cannot explain neither the onset of the canyon-carving nor the full uplift rates. Other, processes have to be explored such as dynamic topography or thermal anomaly beneath the Massif-Central, the magmatism responsible for the important increase in volcanic activity since ~ 6 Myrs (Michon et Merle, 2001; Nehlig et al., 2003) could play a major role, notably in the initiation of Pliocene-Quaternary uplift. Further studies should aim to address the problem of uplift onset, giving more clues concerning the stable continental area but owing the data we presently have, discussing such onset is out of the scope of the paper.

5. Conclusion

Main results of this study are the following three points:

1- Mean incision rate of the Cevennes area is 83 $^{+17}/_{-5}$ m/Ma during the last 4 Ma.

2- This incision is due to regional uplift with higher vertical velocities northward.

3- This uplift is partly due (½ to 2/3) to isostatic adjustment induced by erosion.

Furthermore, our study highlights the importance of multidisciplinary approach especially in the study of low-deformation rate areas.

To the contrary of previous studies that focused on one cave, we have shown that combining karst burial ages and paleomagnetic analysis of clay deposits in several caves over a large elevation range can bring good constraints on incision rates. This multi-cave system approach diminishes the intrinsic limits of the two single methods: low sampling density (and analysis cost) for the TCN ages and difficulty to set the position of paleomagnetic results. Our estimated paleo base level ages are Pliocene-Quaternary (ca. last 4 Ma) and allow to derive a mean incision rate of 83 $^{+17}/_{-5}$ m/Ma for the Cevennes area. The landscape, and especially the river profiles suggest a first-order equilibrium allowing considering the incision rate as an uplift rate.

We have shown using a geomorphological analysis that at least south of the Cévennes, several surfaces are tilted toward the SSE. This kind of study had been performed before on large structures (Champagnac et al., 2007) or endokarstic markers (Granger et Stock, 2004) but it is the first time that it is performed at such scale with small markers. Numerical modeling yields the same pattern of SSE dipping, allowing more confidence in the geomorphometric results.

Our multi-disciplinary approach brings the first absolute dating of the Cévennes landscapes and suggests that the present-day morphology is partly inherited from the Plio-Quaternary erosion-induced isostatic rebound.

We propose that related erosional isostatic adjustment is of major importance for the understanding of the southern French Massif-Central landscape evolution and explains a large part of the uplift.

At larger scale, we assume that the main conclusion of our study can be extrapolated to the majority of the intraplate orogens. That is to say, once the forces responsible for the initial uplift (e.g. plate tectonics, dynamic topography) fade out, the uplift continue thanks to erosion-induced isostatic adjustment.

An analysis at the scale of the Massif Central is now needed before nailing down our interpretations of the Massif-Central dynamics.

Code and data availability

Surface analysis was performed using QGIS version 2.18, MAtlab® code and IGN DEM (RGE Alti®) 5m). Modeling was performed using ADELI code (Hassani et Chery, 1996; Chéry et al., 2016). Data for TCN and paleomagnetic analysis are provided in the manuscript itself or in supplementary material. Additional informations for geologic background are available at http://infoterre.brgm.fr/ (French Geological Survey data visualizer).

Author contributions

OM, PV and GC did the sampling. GC and DF performed the TCN analysis. PC and OM did the magnetic measurements and interpretations. OM did the surface identification and analysis. OM, PV and JC performed the numerical model. OM, OV, JFR, GC, PC, JC and DF interpreted and wrote the article.

Competing interests

The authors declare that they have no conflict of interest.

Acknowlegdments

We are grateful to ANSTO for providing facilities for chemical extraction for the TCN analysis. We thanks the reviewers for useful remarks and comments that we think help to increase the level of the paper.

References

Arthaud F. et Laurent P.: Contraintes, déformations et déplacements dans l'avant-pays pyrénéen du Languedoc méditerranéen, Godin. Acta, 8, 142-157, 1995.

Audra P., Camus H. et Rochette P.: Le karst des plateaux de la moyenne vallée de l'Ardèche : datation par paléomagnétisme des phases d'évolution plio-quaternaires (aven de la Combe Rajeau). Bull. Soc. Géol. France, 2001, t. 172. N°1, pp. 121-129, 2001.

Balco, G., Stone, J.O., Lifton, N.A., Dunai, T.J., 2008. A complete and easily accessible means of calculating surface exposure ages or erosion rates from Be-10 and Al-26 measurements. Quat. Geochronol. 3, 174–195. 2008.

Barbarand J., Lucazeau F., Pagel M. Et Séranne M.: Burial and exhumation history of the south-eastern Massif Central (France) constrained by en apatite fission-track thermochronology. *Tectonophysics,* 335, 275-290, 2001.

Barruol G. et Granet M.: A Tertiary astenospheric flow beneath the southern French Massif Central indicated by upper mantle seismic anisotropy and related to the west Mediterranean extension. Earth and Planetary Science Letters 202 (2002) 31-47, 2002.

Brichau S., Respaut J.P. et Monié P.: New age constraints on emplacement of the Cévenol granitoids, South French Massif Central, Int J Earth Sci 97:725–738, doi: 10.1007/s00531-007-0187-x, 2007.

Bruxelles L.: Dépôts et altérites des plateaux du Larzac central : causses de l'Hospitalet et de Campestre (Aveyron, Gard, Hérault) Evolution morphogénétique, conséquences géologiques et implcations pour l'aménagement. Université d'Aix-Marseille I, Université de Provence, UFR Sciences géographiques et de l'aménagement. Thèse, spécialité : Milieux physiques méditerranéens, 2001.

Calais, E., Freed, A. M., Van Arsdale, R., & Stein, S. (2010). Triggering of New Madrid seismicity by late-Pleistocene erosion. Nature, 466(7306), 608–611. http://doi.org/10.1038/nature09258

Calais, E., T. Camelbeeck, S. Stein, M. Liu, and T. J. Craig (2016), A new paradigm for large earthquakes in stable continental plate interiors, Geophys. Res. Lett., 43, doi:10.1002/2016GL070815, 2016.

Calvet M., Gunnell Y., Braucher R., Hez G., Bourlès D., Guillou V., Delmas M. et ASTER team: Cave levels as proxies for measuring post-orogenic uplift : Evidence from cosmogenic dating of alluvium-

filled caves in the French Pyrenees. Geomorphology 246 (2015) 617- 633 ; doi : 10.1016/j.geomorph.2015.07.013, 2015.

Camus H.: Vallée et réseaux karstiques de la bordure carbonatée sud-cévenole. Relation avec la surrection, le volcanisme et les paléoclimats. Thèse de doctorat, Université Bordeaux 3, 692 p, 2003.

Champagnac J.D., Molnar P., Anderson R.S., Sue C. et Delacou B.: Quaternary erosion-induced isostatic rebound in the western Alps. Geology, March 2007 ; v.35 ; no. 3 ; p. 195-198, doi : 10.1130/ G23053A.1, 2007.

Champagnac J-D. van der Beek P. Diraison G. et Dauphin S.: Flexural isostatic response of the Alps to increased Quaternary erosion recorded by foreland basin remnants, SE France. Terra Nova, Vol 20, No. 3, 213-220, doi : 10.1111/j.1365-3121.2008.00809.x, 2008.

Chéry J., Zoback M.D. et Hassani R.: An integrated mechanical model of the San Andreas Fault in central and northern California. J. Geophys. Res., 106(B10) :22051. 52,61, 2001.

Chéry, J., Genti, M. And Vernant, P. Ice cap melting and low-viscosity crustal root explain the narrow geodetic uplift of the Western Alps.Geophys. Res. Lett.43,1–8 (2016).

Child D.P., Elliott G., Mifsud C., Smith A.M and Fink D., Sample processing for earth science studies at ANTARES. Nuclear Instruments and Methods in Physics Research Section B Beam Interactions with Materials and Atoms 172(1-4):856-860 doi: 10.1016/S0168-583X(00)00198-1, 2000.

Corbel J.: Les phénomènes karstiques dans les Grands Causses. In : Revue de géographie de Lyon, vol. 29, n°4, pp. 287-315, doi : 10.3406/geoca.1954.1990, 1954.

Dautria J.M., Liotard J.M., Bosch D., Alard O.: 160 Ma of sporadic basaltic activity on the Languedoc volcanic line (Southern France): A peculiar cas of lithosphere-astenosphere interplay. Lithos 120 (2010) 202-222, doi: 10.1016/j.lithos.2010.04.009, 2010

Genti M.: Impact des processus de surface sur la déformation actuelle des Pyrénées et des Alpes. Géophysique [physics.geo-ph]. Université de Montpellier, 2015. Français. Thèse, 2016.

Granet M., Wilson M. et Achauer U.: Imaging a mantle plume beneath the French Massif Central. Earth and Planetary Science Letters 136 (1995) 281-296, 1995.

Granger, D. E., Fabel, D. and Palmer, A.N.: Pliocene-Pleistocene incision of the Green River, Kentucky determined from radioactive decay of comogenic 26Al and 10Be in Mammoth Cave sediments. *GSA Bulletin*; July 2001; v. 113; no. 7; p. 825–836

Granger, D. E., Kirchner, J. W., and Finkel, R. C.: Quaternary downcutting rate of the New River, Virginia, measured from differential decay of cosmogenic 26Al and 10Be in cave-deposited alluvium. Geology; Februrary 1997 ; v. 25 ; no.2 ; p. 107-110, 1997.

Granger D.E., Gibbon R.J., Kuman K., Clarke R.J., Bruxelles L. and Caffee M.W.: New cosmogenic burial ages for Sterkfontein Member 2 Australopithecus and Member 5 Oldowan, Nature Letter 2015, doi: 10.1038/nature14268, 2015.

Granger D.E. and Muzikar P.F.: Dating sediment burial with in situ-produced cosmogenic nuclides: theory, techniques, and limitations. Earth and Planetary Science Letters 188 (2001) 269-281, 2001.

Granger D.E. and Stock G.M.: Using cave deposits as geologic tiltmeters : Application to postglacial rebound of the Sierra Nevada, California. Geophysical Research Letters, vol. 31, L22501, doi : 10.1029/2004GL021403, 2004.

Zupan Hajna N., Mihevc A., Pruner P. and Bosák P. 2010. Palaeomagnetic research on karst sediments in Slovenia. International Journal of Speleology, 39(2), 47-60. Bologna (Italy). ISSN 0392-6672, 2010.

Haq B.U., Herdenbol J. and Vail P.R.: Mesozoic and cenozoic chronostratigraphy and cycles of sea-level change. Society Economic Paleontologists Mineralogists Special Publication, 42, 71-108, Tulsa, Oklahoma. 1988.

Harmand D., Adamson K., Rixhon G., Jaillet S., Losson B., Devos A., Hez G., Calvet M. and Audra P.: Relationships between fluvial evolution and karstification related to climatic, tectonic and eustatic forcing in temperate regions, Quaternary Science Reviews (2017) 1-19, doi : 10.1016/j.quascirev.2017.02.016, 2017.

Hassani R. and Chery J., Anaelasticity explains topography associated with Basin and Range normal faulting. Geology 24(12):1095. doi: 10.1130/0091-7613(1996)024<1095:AETAWB>2.3.CO;2. 1996.

Hill C.A., 1999.. Sedimentology and Paleomagnetism of sediments, Kartchner caverns, Arizona. Journal of Cave and Karst Studies 61(2) : 79-83, 1999.

Husson E.: Intéraction géodynamique/karstification et modélisation 3D des massifs carbonatés : Implication sur la distribution prévisionnelle de la karstification. Exemple des paléokarsts crétacés à néogènes du Languedoc montpelliérain. Sciences de la Terre. Université Montpellier 2- Sciences et techniques du Languedoc, 236 p, 2014.

Kooi H., Cloetingh S. et Burrus J.: Lithospheric Necking and Regional Isostasy at Extensional Basins 1. Subsidence and Gravity Modeling With an Application to the Gulf of Lions Margin (SE France), Journal of Geophysical Research , vol. 97, no. B12, Pages 17,553- 17,571, november 10, 1992.

Leroux E., Rabineau M., Aslanian D., Granjeon D., Droz L. et Gorini C.: Stratigraphic simulations of the shelf of the Gulf of Lions: testing subsidence rates and sea-level curves during the Pliocene and Quaternary. Terra Nova, Vol 26, No. 3, 230-238, doi: 10.1111/ter.12091, 2014.

Lofi J., Rabineau M., Gorini C., Berne S., Clauzon G;, De Clarens P., Dos Reis A.T., Mountain G.S., Ryan W.B.F, Steckler M.S. et Fouchet C.: Plio-Quaternary prograding clinoform wedges of the western Gulf of Lion continental margin (NW Mediterranean) after the Messinian Salinity Crisis., Marine Geology July 2003; 198 (3-4) : 289-317, doi: 10.1016/S0025-3227(03)00120-8, 2003.

Lucazeau F. and Vasseur G.: Heat flow density data from France and surrounding margins, In: V. Cermak, L. Rybach and E.R. Decker (Editors), Tectonophysics, 164 (1989) 251-258

Manchuel K., Traversa P., Baumont D., Cara M., Nayman E. Et Durouchoux C.: The French seismic CATalogue (FCAT-17), Bull Earthquake Eng (2018) 16:2227–2251, doi: 10.1007/s10518-017-0236-1, 2018.

Miallier D., Michon L., Evin J., Pilleyre T., Sanzelle S., et Vernet G.: Volcans de la Chaîne des Puys (Massif Central, France) : point sur la chronologie Vasset-Kilian-Pariou-Chopine. Comptes Rendus Géoscience, Elsevier

Michon L. et Merle O.: The evolution of the Massif Central rift: Spatio-temporal distribution of the volcanism. Bulletin de la Society Geologique de France, 2001, t. 172, n°2, pp. 201-211, dog: 102113/172.2.201, 2001.

Miller, K.G., Kominz, M.A., Browning, J.V., Wright, J.D., Mountain, G.S., Katz, M.E.,Sugarman, P.J., Cramer, B.S., Christie-Blick, N., Pekar, S.F.: The Phanerozoic record of global sea-level change. Science 310, 1293–1298, doi : 10.1126/science.1116412, 2005.

Mocochain L.: Les manifestations geodynamiques –Externes et internes- de la crise de salinité messinienne sur une plate-forme carbonatée peri-méditerranéenne : le karst de la basse ardèche (moyenne vallée du rhône ; France). Thèse de doctorat, Université Aix- Marseille I – Université de Provence U.F.R des Sciences géographiques et de l'aménagement Centre Européen de Recherches et d'Enseignement en Géosciences de l'Environnement., 196 p, 2007.

Molliex S., Rabineau M., Leroux E., Bourlès D.L., Authemayou C., Aslanian D., Chauvet F., Civet F. et Jouët G.: Multi-approach quantification of denudation rates in the Gulf of Lion source-to-sink system (SE-France). Earth and Planetary Science Latters 444 (2016) 101-115, doi : 10.1016/j.epsl.2016.03.043, 2016.

Nehlig P., Boivin P., de Goër A., Mergoil J., Prouteau G., Sustrac G. Et Thiéblemont D.: Les volcans du Massif central. Revue BRGM: Géologues, Numéro Spécial: Massif central, 2003.

Nguyen H. N., Vernant P., Mazzotti S., Khazaradze G. et Asensio E.: 3-D GPS velocity field and its implications on the present-day post-orogenic deformation of the Western Alps and Pyrenees. Solid Earth, 7 ; 1349-1363, 2016, doi : 10.5194/se-7-1349-2016, 2016.

Nocquet J.-M. et Calais E.: Crustal velocity field of western Europe from permanent GPS array solutions, 1996-2001. Geophys. J. Int. (2003) 154, 72-88, doi : 10.1046/j.1365-246X.2003.01935.x, 2003.

Nocquet J.-M., Sue C., Walpersdorf A., Tran T., Lenôtre N., Vernant P., Cushing M., Jouanne F., Masson F., Baize S., Chéry J. and Van der Beek P.A., Present-day uplift of the western Alps, Sci. Rep. 6, 28404; doi: 10.1038/srep28404 (2016).

Olivetti V., Godard V., Bellier O. et ASTER team : Cenozoic rejuvenation events of Massif Central topography (France) : Insights from cosmogenic denudation rates and river profiles. Earth and Planetary Science Letters 444 (2016) 179-191, doi : 10.1016/j.epsl.2016.03.049 0012-821X, 2016.

Ouimet, WB, Whipple, KX, Crosby, BT, Johnson, JP, Schildgen, TF. 2008. Epigenetic gorges in fluvial landscapes. *Earth Surface Processes and Landforms* **33**: 1993– 2009. doi: 10.1002/esp.1650 Epigenetic. 2008.

Rolland Y., Petit C., Saillard M., Braucher R., Bourlès D., Darnault R. Cassol D. Et ASTER Team: Inner gorges incision history: A proxy for deglaciation? Insights from Cosmic Ray Exposure dating (10Be and 36Cl) of river-polished surfaces (Tinée River, SW Alps, France). Earth and Planetary Science Letters, Elsevier, 2017, 457, pp.271 - 281, doi : 10.1016/j.epsl.2016.10.007. <hal-01420882>, 2017.

673 Rovey II C.W., Balco G., Forir M. Et Kean W.F.: Stratigraphy, paleomagnetism, and cosmogenic-
674 isotope burial ages of fossil-bearing strata within Riverbluff Cave, Greene County, Missouri.
675 Quaternary Research (2017), 1-13, doi : 10.1017/qua.2017.14, 2017.
676 Saillard M., Petit C., Rolland Y., Braucher R., BOurlès D.L., Zerathe S., Revel M. Et Jourdon A.: Late
677 Quaternary incision rates in the Vésubie catchment area (Southern French Alps) from in situ-produced
678 ^{36}Cl cosmogenic nuclide dating: Tectonic and climatic implications, J. Geophys. Res. Earth Surf., 119,
679 1121–1135, doi:10.1002/ 2013JF002985. 2014.
680 Sanchis E. et Séranne M.: Structural style and tectonic evolution of a polyphase extensional basin of
681 the Gulf of Lion passive margin : the Tertiary Alès basin, southern France. Tectonophysics 322 (2000)
682 219-242, doi : 10.1016/S0040-1951(00)00097-4, 2000.
683 Sartégou A.: Évolution morphogénique des Pyrénées orientales: apports des datations de systèmes
684 karstiques étagés par les nucléides cosmogéniques et la RPE. Géomorphologie. Thèse de l'Université
685 de Perpignan. Français <NNT : 2017PERP0044>. <tel-01708921> , 2017.
686 Sartégou, A., Bourlès, D. L., Blard, P.-H., Braucher, R., Tibari, B., Zimmermann, L., et al. (2018a).
687 Deciphering landscape evolution with karstic networks_ A Pyrenean case study. Quaternary
688 Geochronology, 43, 12–29. http://doi.org/10.1016/j.quageo.2017.09.005
689 Sartégou A., Mialon A., Thomas S., Giordani A., Lacour Q., Jacquet A., André D., Calmels L.,
690 Bourlès D.L., Bruxelles L., Braucher R., Leanni L. Et ASTER team.: When TCN meet high school
691 students: deciphering western Cévennes landscape evolution (Lozère, France) sin g TCN on karstic
692 networks. Poster 4th Nordic Workshop on Cosmogenic Nuclides. 2018b.
693 Schaller M., von Blanckenburg F., Hovius N. Et Kubik P.W.: Large-scale erosion rates from in situ-
694 produced cosmogenic nuclides in European river sediments. Earth and Planetary Science Letters 188
695 (2001) 441-458, 2001.
696 Séranne M., Benedicto A., Labaum P., Truffert C. et Pascal G.: Structural style and evolution of the
697 Gulf of Lion Oligo-Miocene rifting : role of the Pyrenean orogeny. Marine and Petroleum Geology,
698 Vol. 12, No. 8, pp. 809-820, 1995.
699 Séranne M., Camus H., Lucazeau F., Barbarand J. et Quinif Y.: Surrection et érosion polyphasées de la
700 Bordure cévenole. Un exemple de morphogenèse lente. Bull. Soc. Géol. France, 2002, t. 173, n°2, pp.
701 97-112, 2002.
702 Sibuet J.-C., Srivastava S.P. et Spakman W.: Pyrenean orogeny and plate kinematics. Journal of
703 Geophysical Research: Solid Earth, Vol 109, doi: 10.1029/2003JB002514 , 2004.
704 Spassov S. et Valet J.-P.: Detrial magnetisations from redeposition experiments of different natural
705 sediments. Earth and Planetary Science Letters 351-352 (2012) 147-157, dog:
706 10.1016/j.epsl.2012.07.016, 2012
707 Stewart J. and Watts A.B.: Gravity anomalies and spatial variation of flexural rigidity at mountain
708 ranges. Journal of Geophysical research, vol 102, no. B3, Pages 5327-5352, march 10, 1997, doi:
709 10.1029/96JB03664, 1997.
710 Stock G.M., Granger D.E., Sasowsky I.D., Anderson R.S. et Finkel R.C.: Coomparison of U-Th,
711 paleomagnetism, and cosmogenic burial methods for dating caves : Implications for landscape

712 evolution studies. Earth en Planetary Science Letters 236 (2005) 388-403, doi :
713 10.1016/j.epsl.2005.04.024, 2005.
714 Tarayoun A., Mazzotti S., Gueydan F., Quantitative impact of structural inheritance on present-day
715 deformation and seismicity concentration in intraplate deformation zones, Earth and Planetary
716 Science Letters, Volume 518, 2019, Pages 160-171, ISSN 0012-821X, doi:
717 10.1016/j.epsl.2019.04.043., 2017.
718 Tassy A., Mocochain L., Bellier O., Braucher R., Gattacceca J., Bourlès D.: Coupling cosmogenic
719 dating and magnetostratigraphy to constrain the chronological evolution of peri-Mediterranean karsts
720 during the Messinian an the Pliocene: Example of Ardèche Valley, Southern France. Geomorphology,
721 189 (2013), pp. 81-92, doi: 10.1016/j.geomorph.2013.01.019, 2013.
722 Tauxe L., Steindorf J.L. et Harris A.: Depositional remanent magnetisation: Toward an improved
723 theatrical and experimental foundation. Earth and Planetary Science Letters 244 (2006) 515-529, doi:
724 10.1016/J.epsl.2006.02.003, 2006.
725 Tricart P. : From passive margin to continental collision: A tectonic scenario for the western Alps.
726 American journal of science, Vol. 284, February, 1984, P97-120, 1984.
727 Vernant, P., Hivert, F., Chéry, J., Steer, P., Cattin, R., & Rigo, A. (2013). Erosion-induced isostatic
728 rebound triggers extension in low convergent mountain ranges. Geology, 41(4), 467–470.
729 http://doi.org/10.1130/G33942.1
730
731
732
733
734
735

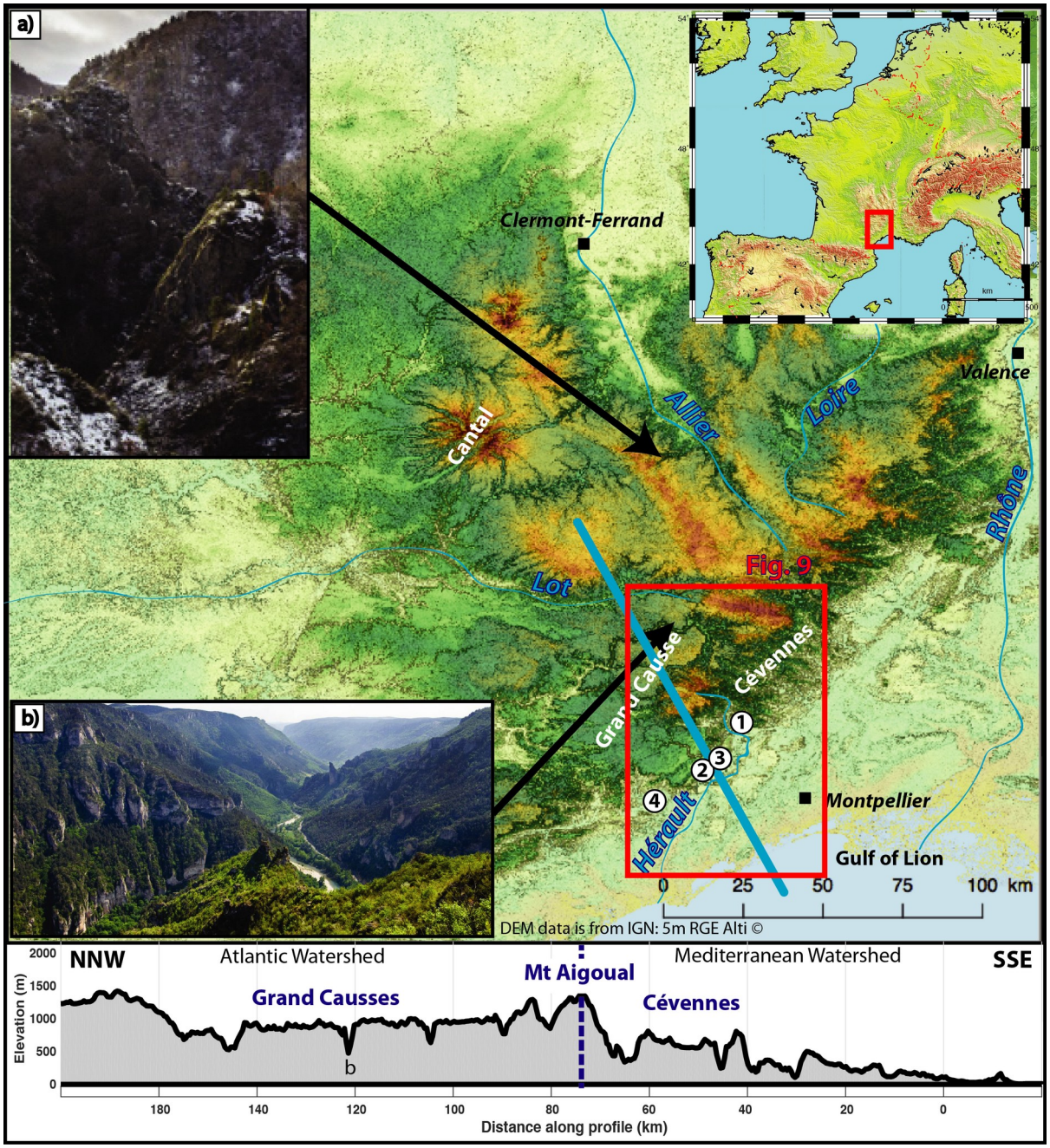

Figure 1: 30 m resolution DEM of the French Massif-Central and slope shadowed. Examples of finite incision typical of the French Massif-Central in a) crystalline basement (Seuge Canyon) and b) limestone plateau (Tarn Canyon). Location of the study area in red box (Fig. 9) and numerated site 1) is the Rieutord Canyon (43,958°N; 3.709°E) where TCN measurements have been done, 2) and 3) are the Leicasse Cave System (43,819°N; 3.56°E),and the Garrel Cave system (43,835°N; 3.616°E) respectively, where paleomagnetic analysis have been done and 4) is the Lodève basin (43,669°N; 3.382°E) with dated basaltic flows. Bottom panel is an example of typical topographic profile used for the numerical model set up.

Note the south-western area with large plateau dissected by canyon, and the rugged area with steep valley called the Cevenne. They are typical regional limestone and crystalline morphology respectively.

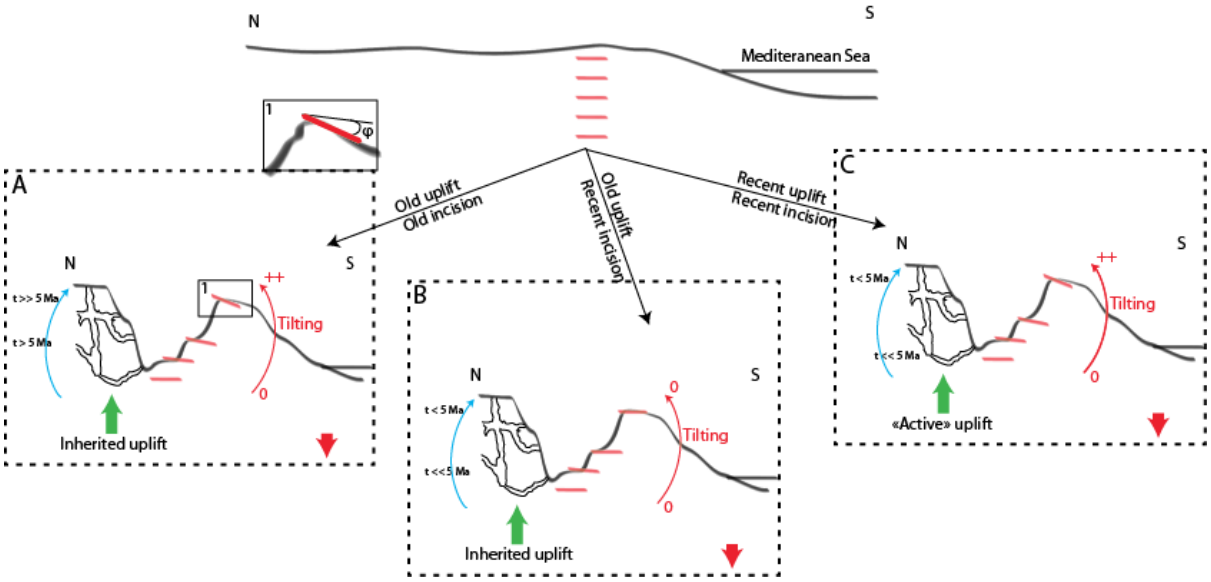

Figure 2: conceptual models for landscape evolution. Top panel is the initial stage (prior to uplift). Each panel represents a possible scenario explaining current morphology: A) Old uplift and old incision, B) Old uplift and recent incision and C) both recent uplift and incision. Blue arrow and associated ages show expected result (or absence of) for burial dating. Red level represents morphological markers that are fossilised when reaching the surface, accumulating afterward (or not) the differential uplift by finite tilting.

Figure 3: Example of quartz cobbles sampled for burial dating. Location: Cuillère Cave (Site 1, Fig.1)

Figure 4: Example of clay sampling for the paleomagnetic study. Location at the entrance shaft (Highest elevation of every samples (~580 m a.s.l.), Leicasse Cave system, Site 2, Fig. 1)

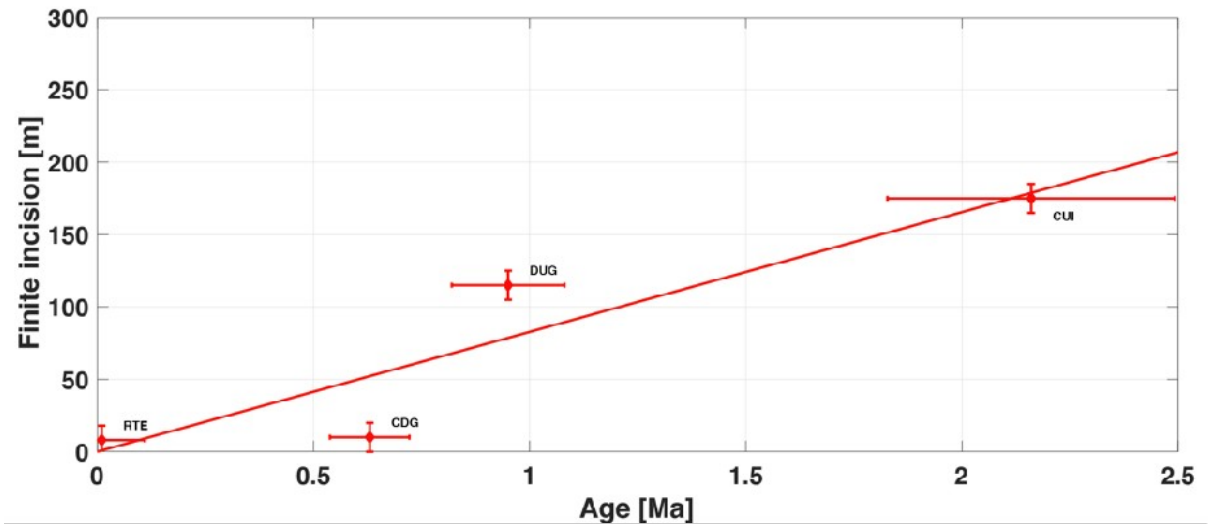

Figure 5: Correlation diagram of finite incision and burial age for the Rieutord canyon (Site 1, Fig. 1). Finite incision is the elevation of the sampling site relatively to the current riverbed. RTE for Route Cave, CDG for Camp de Guerre Cave, DUG for Dugou Cave and CUI for Cuillère Cave

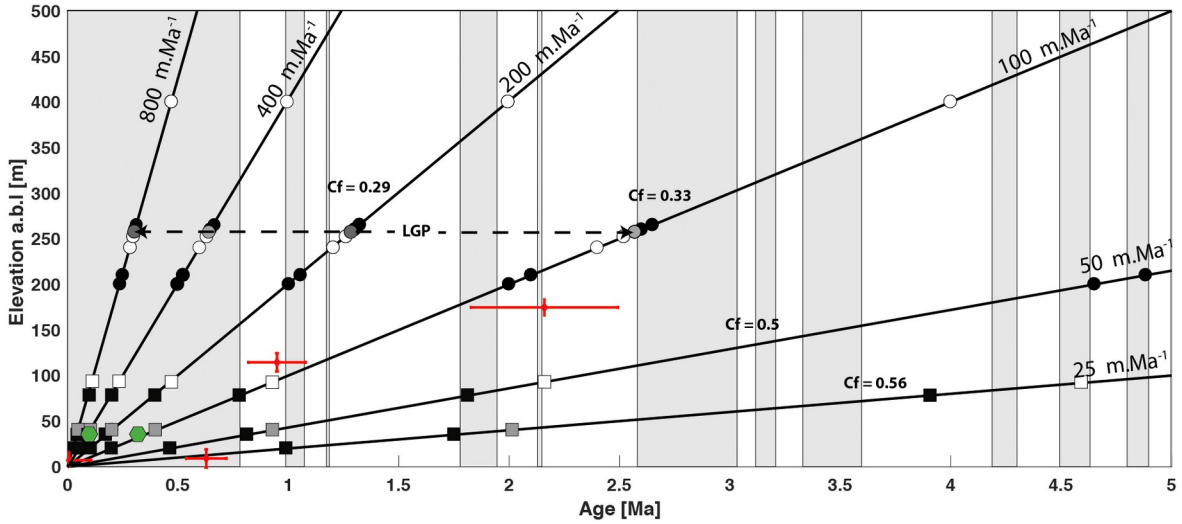

Figure 6. Constraining the incision rate in the Cevennes margin, using paleomagnetic polarities from clay deposits (black, grey and white symbols) and burial ages (red crosses): Circles are from the Leicasse cave with LGP being *les gours sur pattes profile (see text)*, squares are from the Garrel cave. Black, grey and white symbols correspond to normal, transitional and reverse polarities, respectively. Black linear straight lines define possible incision rates that are supposed stable thought time. (numbers in white rectangles define the Cf values are correlation factor between the measured paleomagnetic polarities and the predicted paleomagnetic scale (see also Figure 8). Green hexagons show the U/Th ages obtained on speleothems in the Garrel by Camus (2003).

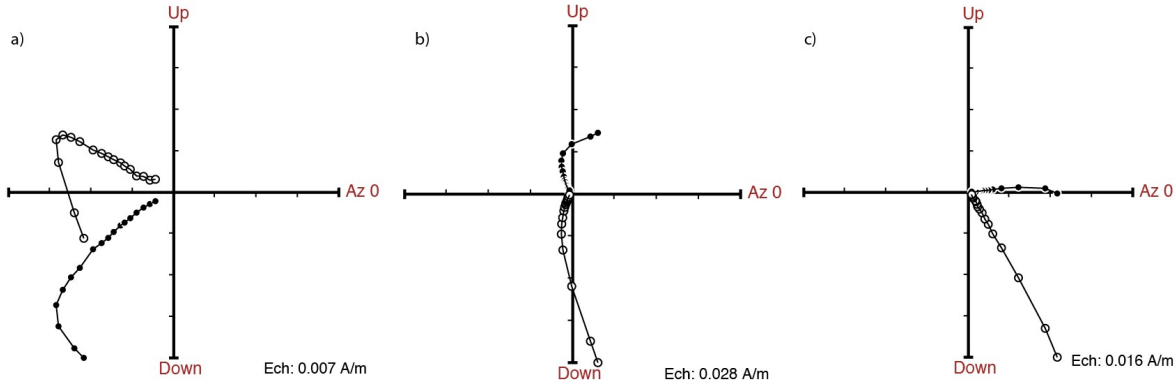

Figure 7: Zijderveld Diagram for three samples from the Gours-sur-Pattes (Leicasse, Site 2, Fig.1) site. Stratigraphical order is from a) (the older, base of the profile) to c) (the younger, top of the profile).

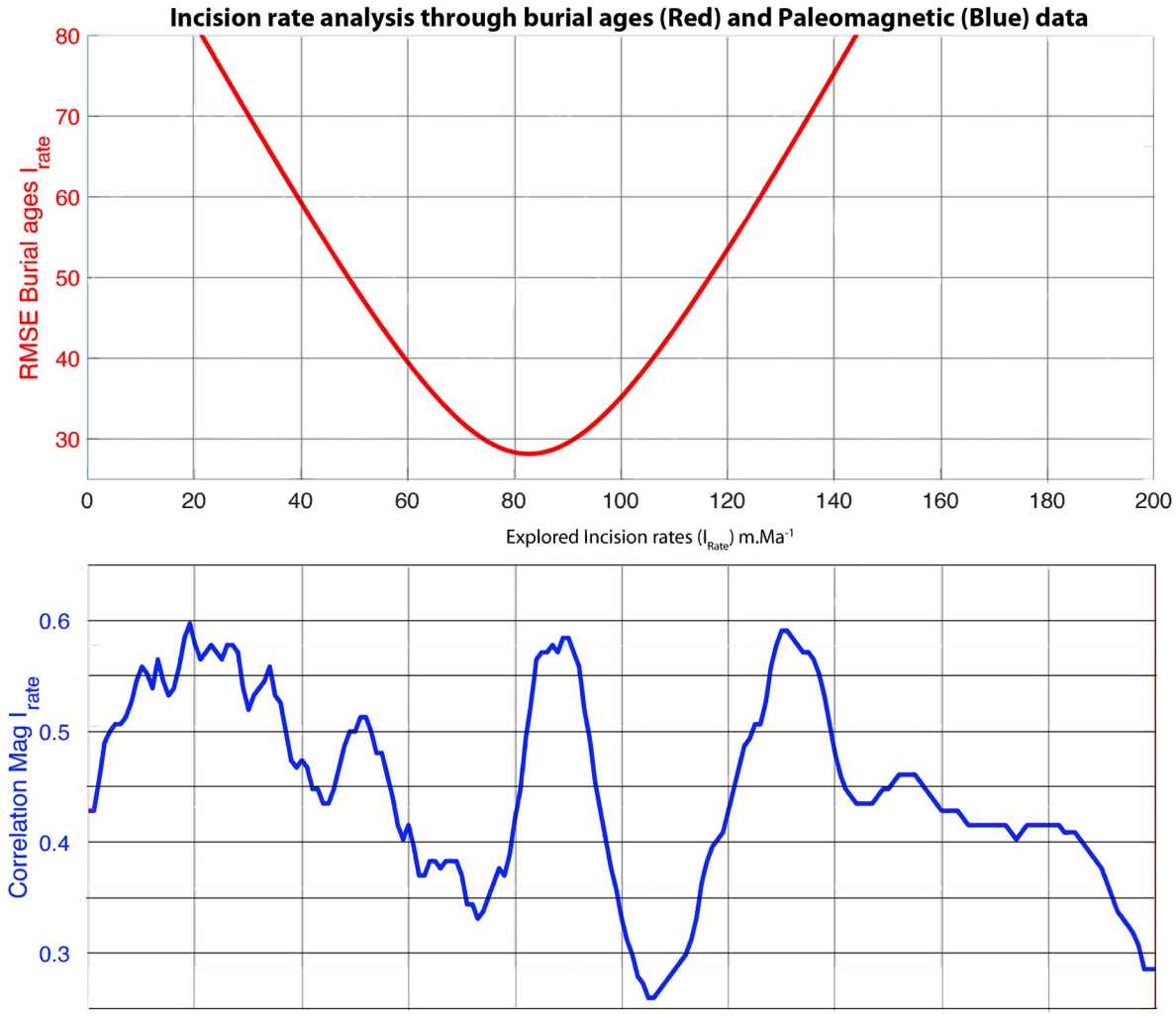

Figure 8: Best incision rates based on paleomagnetic data (blue) and burial ages (red). The blue curve is the normalized smoothed (10 m/Ma sliding window for better visualization) correlation between theoretical and observed polarities. The highest correlation corresponds to the best incision rates. The red curve is the RMSE for the linear regression through the burial ages data set shown on Fig. 4.

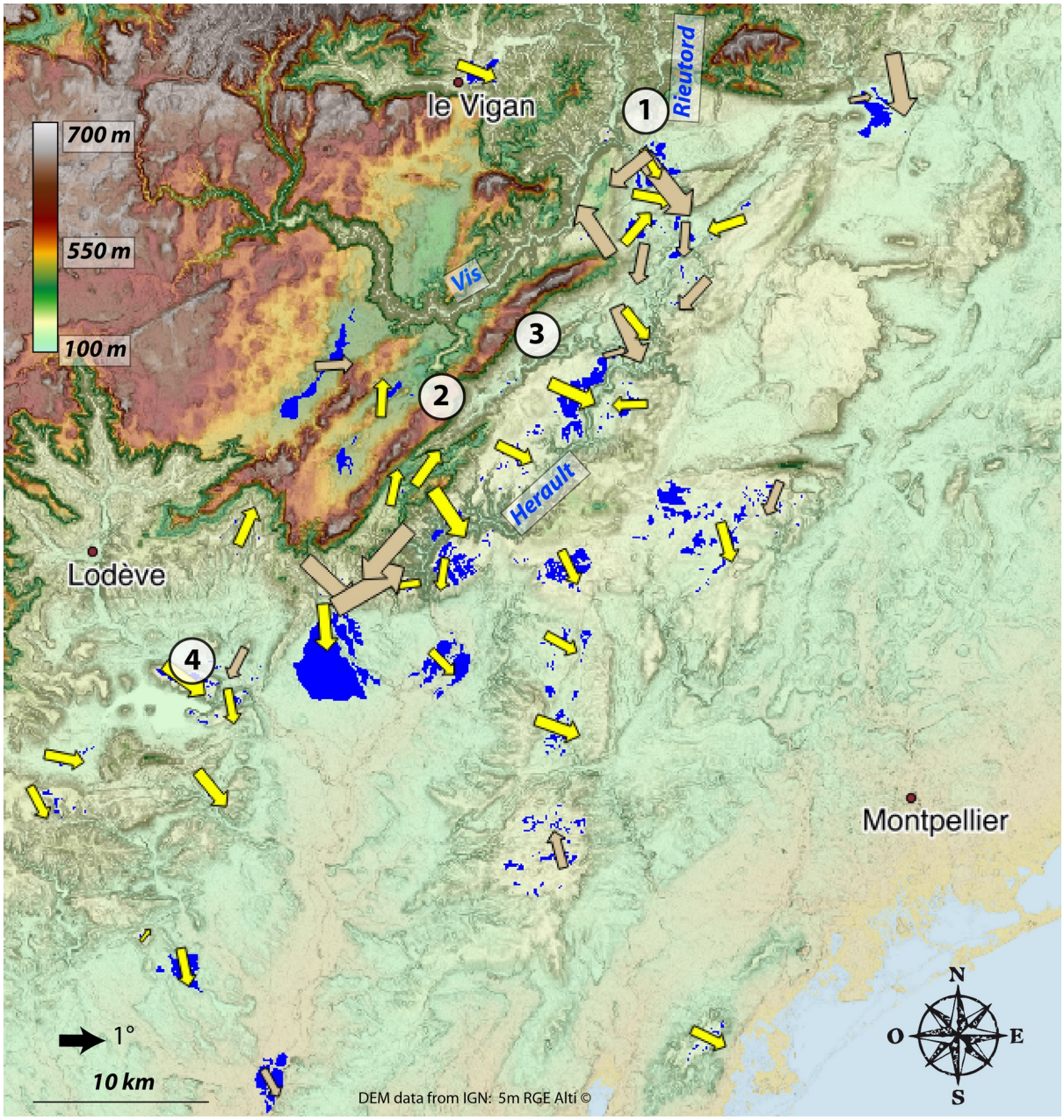

Figure 9: Tilting map of geomorphological benchmark (blue areas). Base-map is 30 m resolution DEM with slope shadow. Arrows are orientated according to the marker downward dip. The arrow size is set accordingly to the corrected tilting angle (the bigger, the more the tilting). Yellow and brown arrows are for robust and less robust surfaces respectively. Several arrows are hidden because of their small size and too high proximity with bigger ones. Numerated site 1) is the Rieutord Canyon, 2) is the Leicasse Cave System, 3) is the Garrel Cave system and 4) is the Lodève basin with dated basaltic flows. See Fig. 1 for geographical coordinates.

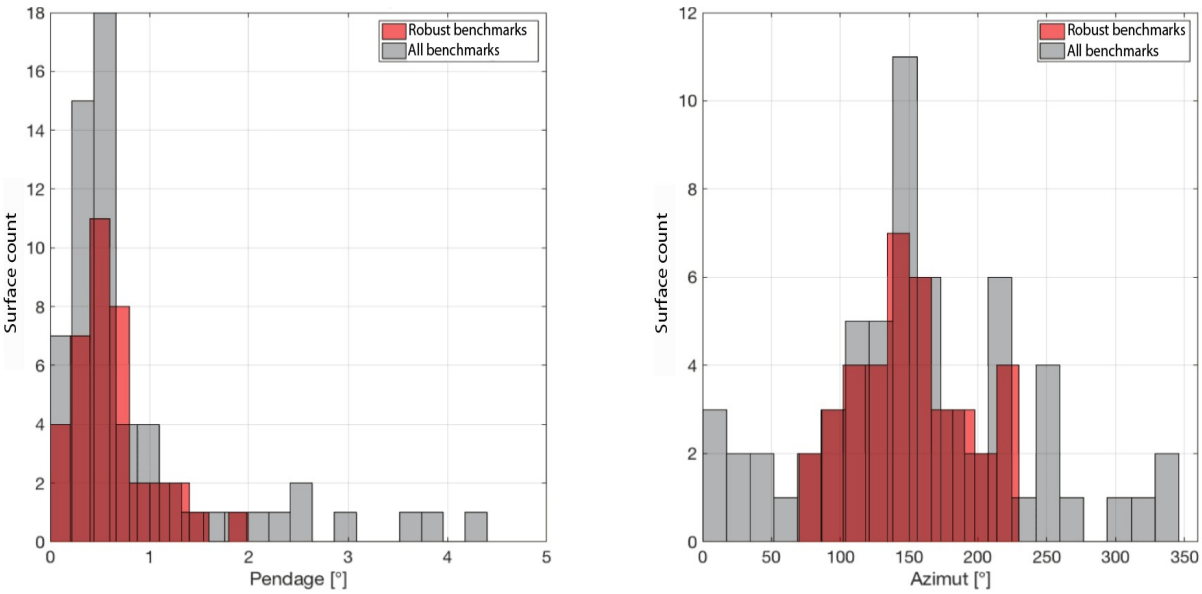

Figure 10: Tilting and azimuth distribution. Left panel is density distribution for surface maximum tilting in degree. Right panel is azimuth of maximum dipping relative to the north. For each histogram, red and grey populations are for robust and primary detected markers.

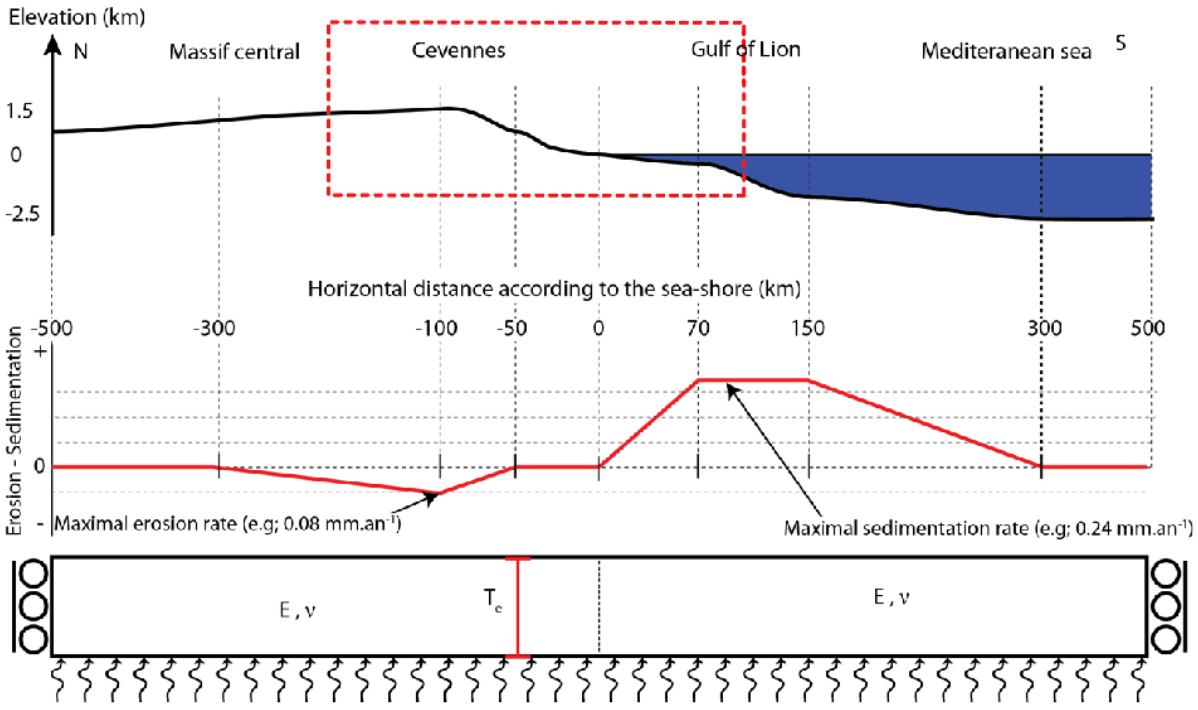

Figure 11: Top panel: schematic topographic profile. The red box delimits the area shown Fig. 1 and 9. Middle panel, surface processes profile, negative values are for erosion and positive values for sedimentation. Bottom panel: model set-up with two compartments (one for the Cevennes area and the second one for the gulf of Lion). The base of the model is compensated in pressure and the right and left limits are fixed at zero horizontal velocity and free vertical velocity. Te is the equivalent elastic thickness (in km), E (Pa) and v are the Young modulus and the Poisson coefficient respectively whom values are independent in each compartment.

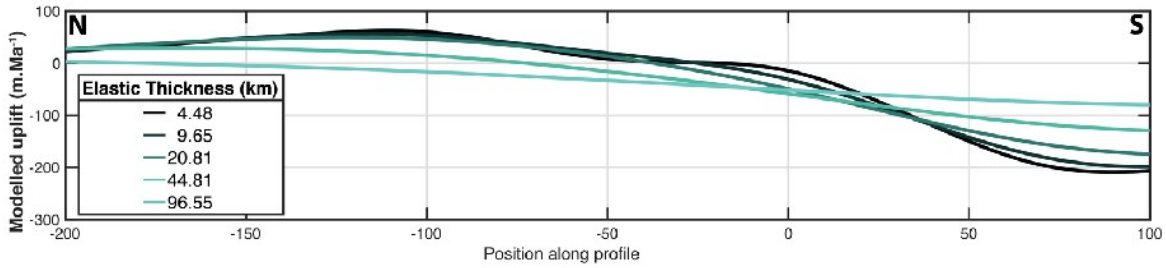

Figure 12: Modeled uplift according to different Te. Most plausible Te are between 10 and 30 km.

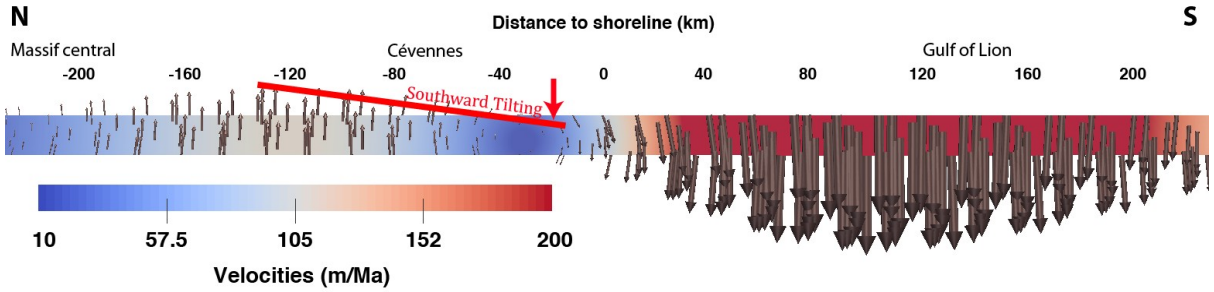

Figure 13: Modeling result for Te= 15 km. Erosion-sedimentation rate profile is the same as in Fig. 6. Velocity field is shown using arrow for orientation velocity magnitudes are quantified by the font color code. Black values on top are distance relative to the sea-shore (positive value landward and negative values seaward). Red line represents the southward modeled tilting due to differential uplift.

Cave	Lat	Lon	Elevation	Height	Conc ^{10}Be (10^4 atm/g)	σ ^{10}Be (10^3 atm/g)	Conc ^{26}Al (10^5 atm/g)	σ ^{26}Al (10^4 atm/g)	^{26}Al/^{10}Be (and σ)	Burial age and σ (Ma)
RTE	43.960	3.707	175	8	3.54	1.18	2.16	1.47	6.11 ± 0.46	0.20 ± 0.15
CDG	43.955	3.710	185	10	8.87	3.12	4.29	3.28	4.83 ± 0.41	0.67 ± 0.16
DUG	43.957	3.711	245	115	1.27	5.68	0.529	0.636	4.15 ± 0.53	0.99 ± 0.25
CUI	43.959	3.711	354	175	1.70	7.14	0.375	0.528	2.20 ± 0.32	2.28 ± 0.28

Table 1: Samples analytical results and parameters. Cave code are: RTE for the "de la route" Cave, CDG for the "Camp de Guerre" cave, DUG for the "Dugou" Cave and CUI for the "Cuillère" Cave. Main parameters are the geographical coordinate (Lat, Lon in decimals degree), the elevation (a.s.l), the height (a.b.l., computed relatively to the surface river elevation. The concentration (atoms/g quartz) of ^{10}Be and ^{26}Al in collected sand samples are all AMS ^{10}Be/Be and ^{26}Al/Al isotopic ratios corrected for full procedural chemistry blanks and normalized to KN-5-4 and KN -4-2, respectively. The error in the brackets is for total analytical error in final average ^{10}Be and ^{26}Al concentrations based on statistical counting error s in final ^{10}Be/Be (^{26}Al/Al) ratios measured by AMS in quadrature with a 1% error in ^{9}Be spike concentration (or a 4% error in ^{27}Al assay in quartz) and a 2% (or 3%) reproducibility error based on repeat of AMS standards. Burial age (minimum) assuming no post-burial production by muons at given depth (all deeper than 30m) in cave below surface and assuming initial ^{26}Al/^{10}Be ratio is given by the production ratio of 6.75. The burial age error determined by using a +/-1σ range in the measured ^{26}Al/^{10}Be ratio